

# Network archaeology: phase transition in the recoverability of network history

Jean-Gabriel Young<sup>a,b,1</sup>, Laurent Hébert-Dufresne<sup>a,c,d</sup>, Edward Laurence<sup>a,b</sup>,  
Charles Murphy<sup>a,b</sup>, Guillaume St-Onge<sup>a,b</sup>, and Patrick Desrosiers<sup>a,b,f</sup>

<sup>a</sup>Département de physique, de génie physique, et d'optique, Université Laval, Québec (QC), G1V 0A6, Canada

<sup>b</sup>Centre interdisciplinaire de modélisation mathématique de l'Université Laval, Québec (QC), G1V 0A6, Canada

<sup>c</sup>Department of Computer Science, University of Vermont, Burlington, VT, 05405, USA

<sup>d</sup>Vermont Complex Systems Center, University of Vermont, Burlington, VT, 05405, USA

<sup>f</sup>Centre de recherche de CERVO, Québec (QC), G1J 2G3, Canada

<sup>1</sup>Corresponding author: [jean-gabriel.young.1@ulaval.ca](mailto:jean-gabriel.young.1@ulaval.ca)

March 28, 2018

## Abstract

Network growth processes can be understood as generative models of the structure and history of complex networks. This point of view naturally leads to the problem of network archaeology: Reconstructing all the past states of a network from its structure—a difficult permutation inference problem. In this paper, we introduce a Bayesian formulation of network archaeology, with a generalization of preferential attachment as our generative mechanism. We develop a sequential importance sampling algorithm to evaluate the posterior averages of this model, as well as an efficient heuristic that uncovers the history of a network in linear time. We use these methods to identify and characterize a phase transition in the quality of the reconstructed history, when they are applied to artificial networks generated by the model itself. Despite the existence of a no-recovery phase, we find that non-trivial inference is possible in a large portion of the parameter space as well as on empirical data.

## 1 Introduction

Unfair distributions of resources are ubiquitous in the natural world. Wealth, sexual activities and attention are all common examples of assets that are concentrated in the hand of the few [1]. While inequalities abound in many contexts, their impact is particularly dramatic in complex networks, whose structure is heavily constrained in the presence of skewed distributions. For instance, the aggregation of edges around a few hubs determines the outcome of diseases spreading in a population [2], the robustness of technological systems to targeted attacks and random failures [3], or the spectral property of many networks [4]. It is therefore not surprising that much effort has been devoted to understanding how unfair distributions come about in networks. Satisfactory explanations have often taken the form of constrained growth processes; the rich-get-richer principle [5], sampling space reduction processes [6] and latent fitness models [7] are all examples of growth processes that lead to a heavy-tailed distribution of the degrees.

A common characteristic shared by these processes is that they do not—nor are they expected to—give a perfect account of reality [8]. Their rules are simple, and only capture the essence of the mechanisms at play, glossing over details. The goal of these models is to better understand broad organizing principles, rather than the random events that completely explain the particulars of an observed network [9]. Thus, large-scale endogenous changes and microscopic variations are all examples of effects that are typically absent in mechanistic models, even if they affect the distribution of resources of real systems.

Despite these simplifications, growth processes endure as useful models of real complex systems. At a macroscopic level, their predictions have often been found to fit the statistics of real networks to surprising degrees of accuracy [5, 10, 11]. At a microscopic level, they have been shown to act effectively as *generative models* of complex networks [12, 13], i.e., as stochastic processes that can explain the details of a network’s structure [14]. This point of view has led, for example, to powerful statistical tests that delineate the role of nodes’ fitness and age in determining a network’s structure [7, 15].

The notion of growth processes as generative model is now being pushed further than ever before. The burgeoning field of *network archaeology* [16], in particular, builds upon the idea that growth processes are generative models of the *history* of complex networks, able to reveal the past states of static systems. This point of view is perhaps the most clearly stated in the bioinformatics literature, which seeks to reconstruct ancient protein–protein interaction (PPI) networks to, e.g., improve PPI network alignment algorithms [17, 18] or understand how the PPI networks of organisms are shaped by evolution [19]. Indeed, almost all algorithmic solutions to the PPI network archaeology problem are based on explicit models of network growth (variations on the duplication–divergence principle), and take the form of parsimonious inference frameworks [19–21]; greedy local searches informed by models [16, 22–24]; or maximum likelihood inference of approximative [25], graphical [18], and Bayesian [26] models of the networks’ evolution.

Less obvious is the fact that a second body of work, rooted in information theory and computer science, also makes the statement that growth processes can generate the history of real complex networks. This second strand of literature [27–34] focuses on temporal reconstruction problems on tree-like networks generated by random attachment processes [5, 35]. It has led thus far to efficient root–finding algorithms with theoretical accuracy guarantees [27–30], and to approximative reconstruction algorithms on trees [31–33]. The former set of algorithms identify the initial subgraph of a randomly grown network, while the latter uncover complete histories (a provably tougher challenge [34]). Applying any of these algorithms to a real network amounts to assuming that growth processes—here random attachment models—are likely generative models.

The goal of the current paper is to directly investigate this notion of random *attachment* processes as generative models of the histories of networks, from the point of view of Bayesian statistics and hidden Markov processes [26]. Our contribution is therefore threefold. One, we give a latent variable formulation of the network archaeology problem, in the context of a generalization of the classical preferential attachment model [5, 36–38]. We derive the full inference procedure associated to this model, including a sampling algorithm for the posterior distribution over the set of all histories, as well as an efficient approximation thereof. Two, we establish the extent to which complete history reconstruction is possible, and, in doing so, identify a phase transition in the quality of the inferred histories (i.e., we find a phase where useful reconstruction is impossible, and a phase where it is achievable in large networks). Our general formulation of the generative models allow us to connect the phase transitions to other known reconstruction results [27, 33]. Three, we demonstrate with numerical experiments that we can extract temporal information from real, static complex networks. We conclude by listing a number of important open problems.

## 2 Results

### 2.1 Bayesian network archaeology

A network  $G$  generated by a growth process is, by construction, associated with a *history*  $X$ , i.e., a series of events (new nodes, new edges) that explains how  $G$  evolved from an initial state  $G_0$ . We consider the loosely defined goal of reconstructing  $X$  as perfectly as possible, using the structure of  $G$  as the only source of information (see Fig. 1). Formally, this is an estimation problem in which the history  $X$  is a latent variable, determined by the structure of the network. The relationship between the network and its history

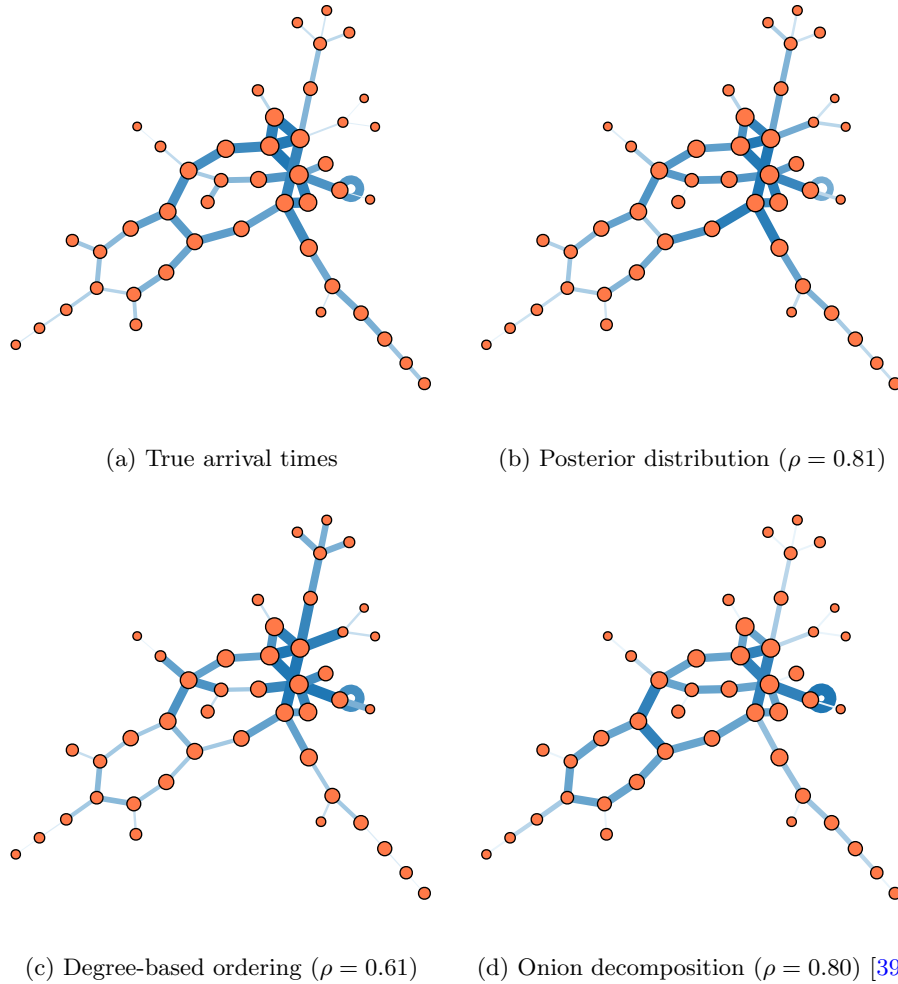


**Figure 1: Reconstructing the history of a growing network.** (a) An artificial network generated by our generalization of the preferential attachment model (with parameters  $\gamma = -1.1, b = 0.9, T = 50$ , see main text). Since the network is artificial, its true history—i.e., the time of arrival of its edges in time—is known. The width and color of edges encode this history; older edges are drawn with thick, dark strokes, whilst younger edges are drawn using thin, light strokes. Likewise, the age of nodes is encoded in their radius. Our goal is to infer these times of arrival as precisely as possible, using the network structure as our only input. The correlation of the true and inferred history is shown below each figure (see Materials and Methods for details). (b) Expected time of arrival, computed with  $10^5$  samples of the posterior distribution of the model, conditioned on the network. (c) Estimated times of arrival constructed by harnessing the correlation between degree and age. (d) Estimated times of arrival prescribed by a recursive removal of low degree nodes, i.e., by the onion decomposition (OD) [39]. The sampling method used to generate the history shown in (a) is, overall, the most accurate, with an average correlation of  $\langle \rho \rangle = 0.81$  over 10 sampling runs (variance  $\sigma = 0.026$ , minimum,  $\rho = 0.75$ , and maximum  $\rho = 0.84$ ). However, it is closely followed by the OD ( $\rho = 0.80$ ), which performs extremely well on sparse networks, due to its ability to identify intrinsically unorderable sets of edges (c.f. the three topmost edges).

is expressed using Bayes’ formula as:

$$P(X|G, \theta) = \frac{P(G|X, \theta)P(X|\theta)}{P(G|\theta)}, \quad (1)$$

where it is assumed—for now—that the parameters  $\theta$  of the growth process are known, or that they can be estimated separately.

To appropriately define the probabilities appearing in Eq. (1), it is crucial to notice that there are two categories of histories, given a network  $G$ : Those that are *consistent* with  $G$  (also called the feasible [33] or compatible [23] histories of  $G$ ), and those that are not. A history is consistent with a network if it has a non-zero probability, however small, of being the *true* history of the network according to the selected growth model. Consistency, in short, is a model-dependent statement. There are obviously many histories consistent with any given network—possibly infinitely many [20]—, but only one network corresponds to any given history. Therefore, the notion of consistency implies that the likelihood  $P(G|X, \theta)$  acts as a logical variable: It equals one if and only if the history  $X$  is consistent with the observed network  $G$ , and it is equal to zero otherwise. In turn, this implies that the evidence  $P(G|\theta)$  appearing in the denominator of Eq. (1) is a sum of  $P(X|\theta)$  over all histories consistent with  $G$ . A complete specification of the probabilities is obtained upon choosing a growth process; this allows for the calculation of  $P(X|\theta)$ , often as a product of transition probabilities.

In this latent variable formulation of the network archaeology problem, reconstructing the past amounts to extracting information from the  $G$  via the posterior distribution  $P(X|G, \theta)$ . Doing so is not as straightforward as it first appears. The posterior distribution may be heavily degenerated, or even uniform over the set of all histories consistent with  $G$ , for some growth processes [34] (see Supplementary Information). Therefore, a useful and attainable goal cannot be to find the one true history  $\tilde{X}(G)$  of  $G$ , because this history is often not identifiable. It turns out that another inference task, with a subtly different definition, is both challenging and achievable: That of finding a history as correlated with the ground-truth  $\tilde{X}(G)$  as possible. We henceforth adopt this maximization as our inference goal. As we will see shortly, the key to success is the fact that we can *combine* histories to construct a good estimate of  $\tilde{X}(G)$ .

## 2.2 Random attachment model

For the sake of concreteness, we will discuss of network archaeology in the context of a specific growth process that generalizes the classical PA model. More precisely, we will use a variant that incorporates both a non-linear attachment kernel [37] and densification events, i.e., attachment events between existing nodes [36, 38, 40, 41]. But let us emphasize that the scope of the network archaeology is broader; changing the specifics of the growth processes only affects how the probabilities  $P(X|\theta)$  are computed, and how they are optimally sampled (see for example Ref. [26] for a related treatment of a duplication–divergence model).

With this in mind, in the considered model, a new undirected edge is added at each time step, starting from some initial network  $G_0$ , which we choose to be a single edge. With probability  $1 - b$  the edge connects two existing nodes, and it connects an existing node to a new node with complementary probability  $b$ . Whenever an existing node is involved at time  $t + 1$ , it is chosen randomly with probability proportional to  $k_i^\gamma(t)$ , where  $k_i(t)$  is the degree of node  $i$  at time  $t$ , and  $\gamma$  is the exponent of the attachment kernel.

The parameter  $b \in [0, 1]$  controls the density, and  $\gamma \in \mathbb{R}$  controls the strength of the rich-get-richer effect (see Fig. 2). We refer to these parameters collectively with  $\theta = (\gamma, b)$ . We recover the classical PA model with  $(\gamma = 1, b = 1)$ , the random attachment model with  $(\gamma = 0, b = 1)$  [35], and an undirected version of the Krapivsky-Redner-Leyvraz generalization [37] if  $\gamma$  is free to vary and  $b = 1$ . The model technically generates multigraphs for any  $b$  smaller than one, although the number of redundant edges and self-loops is vanishing for all  $b$  in the large network limit when  $\gamma < 1$ . It is thus a reasonable model of multigraphs, but also a good approximation of large, sparse networks, with few or no redundant edges and self-loops.

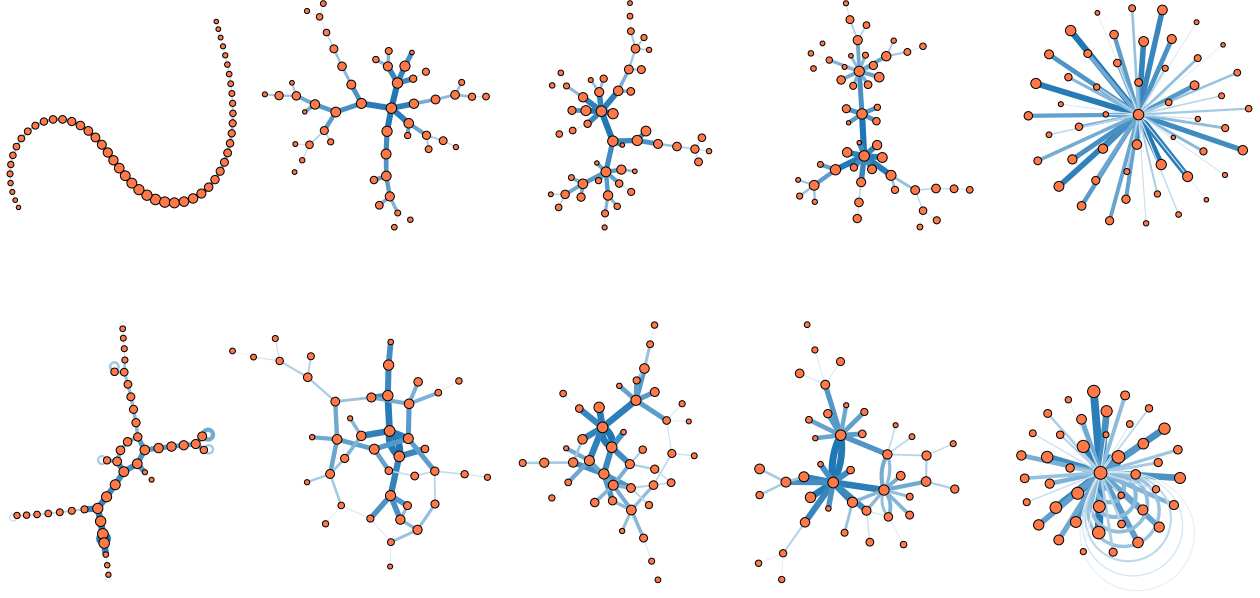


Figure 2: **Network zoo**. Examples of networks generated by the process with  $b = 1$  (top row) and  $b = 0.75$  (bottom row), and  $\gamma \in \{-10, -1, 0, 1, 10\}$  (from left to right). As in Fig. 1, the color and size of an edge indicates its arrival time, and likewise for the nodes.

### 2.3 Inference algorithms

Every event marks the arrival of precisely one new edge in the model. This allows us to represent histories compactly as an ordering of the edges of  $G$  in discrete time  $t = 0, \dots, T - 1$ , an arbitrary time-scale defined in terms of events [1]. Estimating the history then amounts to estimating the arrival times  $\tau_{\tilde{X}}(e)$  of the edges  $e \in E(G)$  in the ground-truth history  $\tilde{X}$ , and the quality of a reconstructed history  $\hat{X}$  is naturally quantified by its Pearson product-moment correlation with the ground-truth.

The optimal estimator  $\hat{\tau}(e)$  of the arrival time of edge  $e$  is the posterior average (see Supplementary Information):

$$\hat{\tau}(e) = \langle \tau_X(e) \rangle = \sum_{X \in \Psi(G)} \tau_X(e) P(X|G, \theta), \quad (2)$$

where  $\Psi(G)$  is the set of histories consistent with  $G$ . This estimator effectively combines histories, overcoming the degeneracy of the posterior distribution. It is straightforward to show that this average minimizes the expected mean-squared error (MMSE) on  $\tau_{\tilde{X}}(e)$ , and we therefore refer to it as the MMSE estimator of the arrival time. Unfortunately, calculating the complete set of MMSE estimators  $\{\langle \tau_X(e) \rangle\}$  is costly, because there are far too many histories consistent with networks of even moderate sizes. Hence, we resort to approximations.

We consider algorithms that fall in two broad categories: Sampling methods, whose goal is to evaluate Eq. (2) directly, but also topological methods that only rely on the structure of  $G$  to make predictions, forgoing explicit knowledge of the posterior distribution  $P(X|G, \theta)$ . Methods in the first category are the most accurate, but they are also more computationally demanding than, say, a simple sort based on the degree.

With sampling methods, our goal is to generate random histories  $\{x_i\}_{i=1, \dots, n}$  to approximate averages taken over  $P(X|G, \theta)$ . The most notable characteristic of this distribution is that its support  $\Psi(G)$  only contains histories describing a growing network that is connected at all steps [the  $(\gamma, b)$  generalization of PA

never generates disconnected components]. This constraint makes sequential importance sampling [26, 42, 43] an ideal choice, because it can explicitly enforce connectedness in the histories. Importance sampling relies on the transformation

$$\begin{aligned}
\langle f(X) \rangle_P &:= \sum_{X \in \Psi(G)} P(X|G, \theta) f(X) \\
&= \sum_{X \in \Psi(G)} \frac{P(X|G, \theta) f(X)}{Q(X|G)} Q(X|G) \\
&\approx \frac{1}{n} \sum_{i=1}^n \frac{P(x_i|G, \theta) f(x_i)}{Q(x_i|G)},
\end{aligned} \tag{3}$$

where the  $n$  samples  $\{x_i\}_{i=1, \dots, n}$  are drawn i.i.d. from a proposal distribution  $Q(X|G)$  different from  $P(X|G, \theta)$ . The idea is to use the proposal distribution to harness known properties of the target distribution—here the connectedness of growing networks. With efficiency in mind, we opt for a random recursive enumeration of the edges of  $G$ , associated to probabilities  $Q(x_i|G)$  that can be easily computed on-the-fly, at no additional computational cost (see Materials and Methods). This proposal distribution—known as snowball sampling [44]—generates connected histories in linear time, i.e., in  $O(|E| \times k_{\max})$  steps where  $k_{\max}$  is the maximal degree.

With topological methods, our goal is to obtain a baseline performance, but also to investigate just how much information can be extracted without using sophisticated sampling methods. We consider two methods of linear complexity in the number of edges in the network. Both methods generate rankings of the nodes, and we use these rankings to induce a ranking on the edges, declaring ties when a pair of edges cannot be ordered [33]. First, since age correlates with the degree in random attachment processes [5, 45], we consider a simple ordering of the edges by the degree of their nodes. Second, because edges closer to the center of a network are more likely to be old [46], we also use a method that harnesses the network’s structure: the onion decomposition (OD) [39], a refinement of the  $k$ -core decomposition algorithm [47, 48] that split the network into layers, from peripheral leaves to central nodes. A closely related “peeling” method has been recently introduced in Ref. [33] to tackle the archaeology problem in the case ( $\gamma = 1, b = 1$ ).

## 2.4 Inference on artificial trees

We begin by testing the inference algorithms on trees drawn from the generative model itself (i.e., we set  $b = 1$  and consider that  $\gamma$  is a free parameter). Because these networks are artificial, we have access to the ground-truth, and we can therefore compute the correlation of the reconstructed and true histories.

The average achieved correlation is shown as a function of the attachment kernel  $\gamma$  in Fig. 3 (a), on small networks ( $T = 50$ ). We distinguish two regimes based on the performance of the degree estimators: The regime  $\gamma > 0$ , characterized by skewed distributions of degrees, and the homogeneous regime  $\gamma < 0$ . The three methods behave similarly in the former regime: They first yield a relatively large correlation at  $\gamma = 0$ , and their quality then quickly plummet with growing  $\gamma$ , ultimately converging to a null average correlation for sufficiently large values of  $\gamma$ . Throughout this transition, the MMSE estimators remain slightly superior to the OD estimators, and they both outperform the degree estimators by a significant—albeit constant—margin. The correlation gap is, in contrast, much larger in the homogeneous regime. While the quality of the OD and MMSE estimators increases with decreasing  $\gamma$ —reaching near perfection when  $\gamma \ll 0$ —, the correlation achieved by the degree estimators actually goes in the opposite direction and shrinks with  $\gamma$ . As we will show in the Discussion, this discrepancy can be understood in terms of phase transitions in the generative model [37].

A better numerical portrait of the phase transition is shown in Fig. 4 (a), where we apply the efficient and nearly optimal OD method to increasingly larger networks. We find that for most values of  $\gamma > 1$ , the

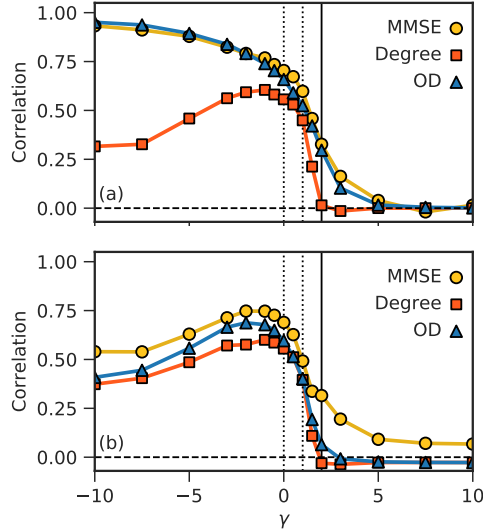


Figure 3: **Phase transition in the quality of the reconstruction.** Average correlation attained by the minimum mean-squared error (MMSE) estimators and two efficient methods based on network properties (a degree based method and the onion decomposition [39]), on artificial networks of  $T = 50$  edges generated using our generalization of the preferential attachment model. **(a)** Phase transition for tree-like networks generated with  $b = 1$ . The special points corresponding to the uniform attachment model and the classical preferential attachment model are indicated with dotted vertical lines, at  $\gamma = 0$  and  $\gamma = 1$ . The point where infinitely large networks fully condensate is shown with a solid vertical line at  $\gamma = 2$  [37]. **(b)** Typical diagram for networks with cycles, here at  $b = 0.75$ . Each point is obtained by averaging the correlation obtained on 25 different network instances. We use  $n = 5 \times 10^6$  samples to evaluate the MMSE estimators and a seed bias of  $\alpha = 5$  (see Materials and Methods).

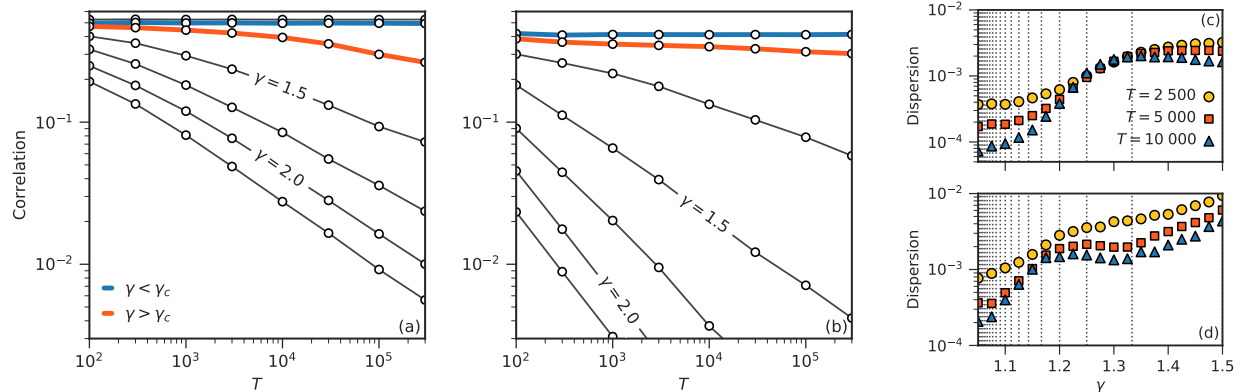


Figure 4: **Detail of the phase transition, through the lens of the OD.** (a,b) Finite-size scaling analysis of the phase transition of Fig. 3. The average correlation attained by OD is shown against the size of networks generated with (a)  $b = 1$  and (b)  $b = 0.75$ , for  $\gamma \in \{1.00, 1.10, 1.25, 1.50, 1.75, 2.00, 2.25\}$  (from top to bottom). Curves that lie over (orange) and below (blue) the observed critical  $\gamma_c$  are highlighted. (c,d) Dispersion of the correlation, as a function of  $\gamma$  in small networks generated with (c)  $b = 1$  and (d)  $b = 0.75$ . The dispersion quantifies the relative concentration of the inference results; it is defined as the variance of the correlation divided by its mean. Vertical dotted lines indicate the important transitions of the generative model. The region to the right of  $\gamma_m = (m + 1)/m$  is characterized by a finite number of nodes of degree strictly superior to  $m$  (in the case  $b = 1$ ) [37].

average correlation attained by the OD decreases as  $T^{-\delta(\gamma)}$  with  $\delta(\gamma) > 0$ . If  $\gamma$  is close enough to 1, however, we do not observe any variations, suggesting that non-trivial inference is possible in infinite networks (similar results hold for  $\gamma < 1$ , not shown). Figure 4 (c) sheds additional light on these two qualitative regimes; it shows that the dispersion of the inference results decreases with growing network sizes, for  $\gamma$  close to 1 and  $3/2$ , but that there is a region in between where the dispersion is independent of  $T$ . This region is aligned with the onset of robust inference [according to Fig. 4 (a)], signaling a potential phase transition at some  $\gamma_c > 1$ .

## 2.5 Inference on artificial networks with cycles

It is clear that trees offer an easier challenge than perfectly general networks, because long-range loops (i) drastically increase the number of histories consistent with  $G$ , and (ii) introduce uncertainties in the ordering of large subsets of edges. To get a better understanding of the model, we therefore repeat the above numerical experiments on more general networks that include cycles, generated with  $b < 1$ . The outcome of our experiments are summarized in Fig. 3 (b) and Figs. 4 (b,d).

Allowing for cycles leads to three notable differences. First, we find that perfect reconstruction is no longer possible in the  $\gamma < 0$  regime. Second, the separation between the MMSE estimators and the topological methods (OD, degree) becomes more significant for all  $\gamma$ . Third and finally, the transition becomes sharper and it occurs at a lower value of  $\gamma_c(b)$ ; notice the much sharper decline in Fig. 4 (b), and the fact that the region where the dispersion is independent from  $T$  shifts to lower values of  $\gamma$  [c.f. Fig. 4 (d)].

## 2.6 A different task: root-finding

Inferring the complete history  $\tilde{X}$  is only one of many possible network archaeology task that fits within the Bayesian formulation of network archaeology. As an example of its versatility, we consider another related

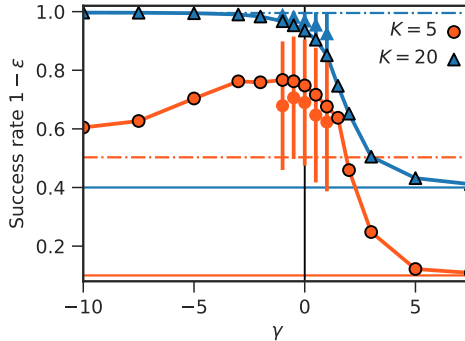


Figure 5: **Root-finding on artificial trees.** Success rate of the root-finding algorithms, with sets  $\mathcal{R}$  of sizes  $K = 5$  and  $K = 20$  on artificial networks of  $T = 50$  edges. The results of OD are shown with solid lines and closed symbols, while the sampling results are shown with open symbols and error bars of one standard deviation. The horizontal solid lines show the accuracy associated to randomly constructed sets  $\mathcal{R}$  (no information retrieval), while the horizontal dotted lines shows the expected success rate in the limit  $\gamma \rightarrow -\infty$  (see Discussion). Sampling is not nearly as efficient as using OD for this problem, so we only compute them for  $\gamma \in \{-1, -\frac{1}{2}, 0, \frac{1}{2}, 1\}$ , with  $n = 10^6$  samples. More samples are required to evaluate the set  $\mathcal{R}$  correctly, which explains the large variance and poorer results of  $K = 5$ .

problem, that of finding the root—i.e., the first edge—of  $G$  [30]. Consider for example the problem of finding the root—i.e., the first edge—of  $G$  [30]. In line with Refs. [27–29], we can give a solution to this problem in terms of *sets*: we define a procedure that returns a set  $\mathcal{R}$  of  $K(\varepsilon)$  edges, and guarantee that it will contain the first edge with probability  $1 - \varepsilon$ . The size  $K$  depends on the acceptable error rate  $\varepsilon$ ; larger sets cast a wider net, and are therefore more likely to contain the root.

To compute  $\mathcal{R}$ , we use a strategy based on the marginalization of the distribution  $P(X|G, \theta)$ . We first obtain the probability  $P[\tau_X(e) = 0]$  that an edge  $e$  is the first, for each  $e \in E$ , via

$$P[\tau_X(e) = 0|G, \theta] = \sum_{X \in \Psi(G)} \mathbb{I}[\tau_X(e) = 0] P(X|G, \theta) = \sum_{X \in \Psi_r(G, e)} P(X|G, \theta). \quad (4)$$

where  $\Psi_r(G, e)$  is the set of histories that begin with  $e$  and where  $\mathbb{I}[S]$  is the indicator function, equal to 1 if the statement  $S$  is true, and to 0 otherwise. We then define  $\mathcal{R}$  as the set formed by the  $K$  edges that have the largest posterior probability  $P[\tau_X(e) = 0]$ . This probability is written in the form of Eq. (3) and it is therefore amenable to sampling. For comparison, we also infer the root with the much faster onion decomposition, by constructing  $\mathcal{R}$  with the  $K$  most central edges (with ties broken at random).

The accuracy of the resulting algorithms is shown as a function of  $\gamma$  in Fig. 5. We distinguish, again, two main phases: Accurate reconstruction is possible in the strongly homogeneous regime  $\gamma \ll 0$ , but the success rate diminishes with growing  $\gamma$ , reaching a non-informative limit in the regime  $\gamma \gg 0$ . This, of course, parallels the phase transitions of Figs. 3–4, since a good overall correlation is only achievable if the root can be reliably identified. When  $K \ll T$ , the accuracy peaks at some value of  $\gamma < 0$ , before slowly decreasing to reach a smaller—but still informative—rate of success.

## 2.7 Application: The social network of a research institution

The end goal of network archaeology is to recover temporal information from real temporal networks not *explicitly* generated by growth processes. We here show that our inference methods can uncover the history of a growing social network, captured by email sent within a large European research institution [49]. The

nodes of this network represent the members of the research institution, and they are connected by a time-stamped edge as soon as they have sent enough reciprocated emails, signaling a genuine connection (see Materials and Methods). This gives us access to a ground-truth; our goal is again to guess the complete ground-truth history  $\tilde{X}$  of the largest connected component.

The results of our analysis are summarized in Fig. 6, where we show the real network and compare the inferred histories with the ground-truth. We find estimated histories with correlations  $\rho_{\text{Degree}} = 0.388$ ,  $\rho_{\text{OD}} = 0.409$  and  $\rho_{\text{MMSE}} = 0.615$ . The network contains a dense connected core which is correctly placed first by all methods (the largest central nodes). More errors are made in ordering the periphery, because it contains fewer discriminating features (i.e., it is sparse in temporal information). Confirming that the  $(\gamma, b)$  generalization of PA is a good description of the observed network, we find that its degree distribution passes the standard goodness-of-fit test of Ref. [50].

## Discussion

There are two main themes to this paper: The accuracy of network archaeology on artificial networks—a mathematical problem—and network archaeology as a generative model for real systems—the related statistical tool. We now discuss these topics in turn, beginning with the mathematical aspect of the problem.

### 2.8 Of information and phase transitions

The structure of a network generated by a growth model encodes—literally—its history. In the Results section, we have shown that this history can be recovered to varying degree of accuracy, depending on the mechanisms of the generative model. These variations in accuracy, as we now show, can be largely understood in terms of the qualitative regimes of the underlying generative model.

#### 2.8.1 Model phenomenology

Let us first focus on the special case  $b = 1$  and  $\gamma \in \mathbb{R}$ , thoroughly analyzed in Ref. [37]. This model has many known phases (see Fig. 2), characterized by different degree distributions. In the limit  $\gamma \rightarrow -\infty$ , the model generates long paths, where every node has degree 2 except for the two end-nodes, of degree 1. For all negative values of  $\gamma$ , the precise form of the degree distribution is not known, but it is clear that the model favors degree homogeneity. When  $\gamma = 0$ , the degree distribution is geometric, of mean 2 (since we recover the uniform attachment model [35]). In the interval  $0 < \gamma < 1$ , the degree distribution takes the form a stretched exponential, with an asymptotic behavior fixed by  $\gamma$ . At precisely  $\gamma = 1$ , the attachment kernel becomes linear and the networks scale-free: The degree distribution follows a power-law of exponent  $-3$ . In the interval  $1 < \gamma < 2$ , the networks *condensate* in a rapid succession of phase transitions at  $\gamma_m = (m+1)/m$  for  $m \in \mathbb{N}^*$ . When  $\gamma > \gamma_m$ , the number of nodes of degree greater than  $m$  becomes finite. As a result, an extensive fraction of the edges aggregates around a single node—the condensate—and this fraction grows with increasing  $\gamma$  [51]. The condensation is complete at  $\gamma = 2$ , where the model enters a winner-takes-all scenario characterized by a central node that monopolizes nearly all the edges, with high probability.

#### 2.8.2 Scalable inference and the no-recovery phase

The appearance of a condensate from  $\gamma > 1$  onwards gives a nice qualitative explanation of the phase transition observed in Figs. 3–5. The important insight is that the condensate significantly limit our ability to infer the history of a network, due to the fact that it scales with the system size. When an edge attaches to the condensate, it is effectively wasted because all the edges of a star-graph are structurally equivalent, and

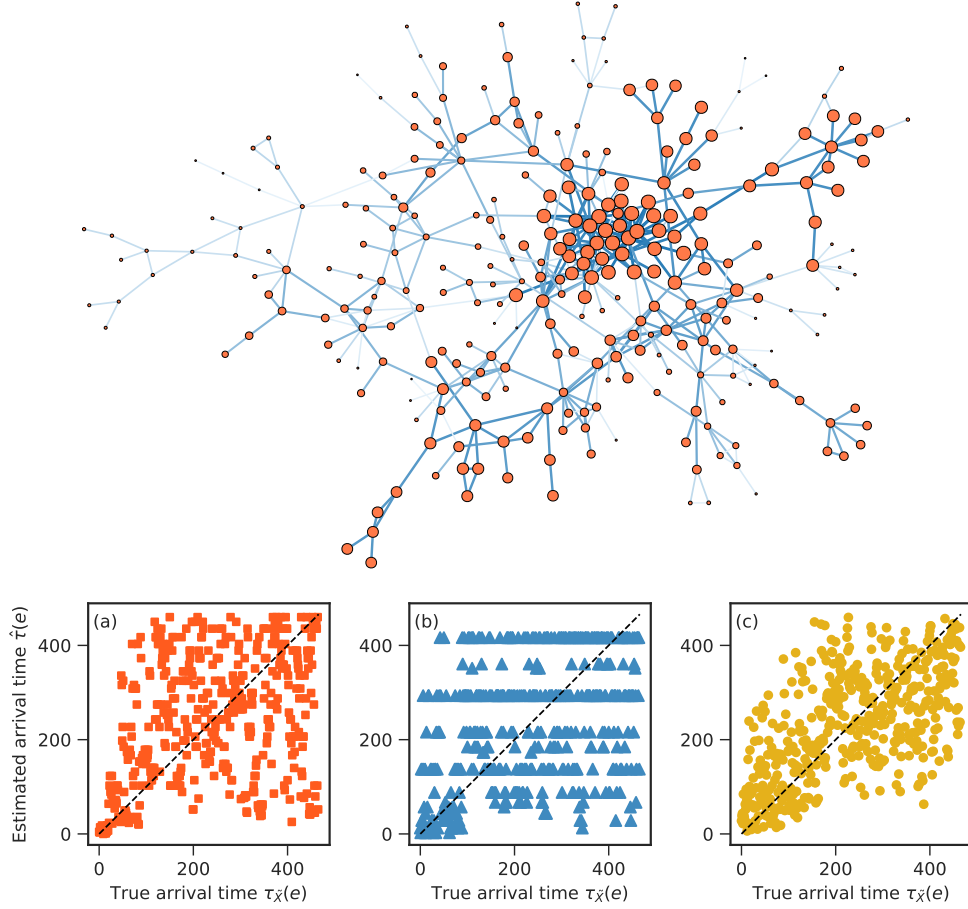


Figure 6: **Application of the inference framework to the giant component of the social network of a large European research institution.** **(top)** Nodes represent the members of the institution [49], and edges represent strong social ties, as captured by numerous email exchanges. Older edges are drawn with thick, dark strokes, whilst younger edges are drawn using thin, light strokes. The radius of a node is proportional to its age. We find that this network is best modeled by  $\hat{b} = 0.63$  and  $\hat{\gamma} = 0.07$ . This pair of parameters is associated to a KS-statistic of  $D^* = 0.040$ , and a significance level of  $P[D > D^*] = 0.24$ , see Materials and Methods. **(bottom)** Inferred arrival time versus true arrival time. A perfect result is shown for reference (diagonal dashed line). The attained correlations are: **(a)**  $\rho_{\text{Degree}} = 0.388$ , **(b)**  $\rho_{\text{OD}} = 0.409$ , and **(c)**  $\rho_{\text{MMSE}} = 0.615$ . The latter is evaluated with  $n = 10^4$  samples.

therefore not orderable. Hence, the diminishing correlation of the estimators in the regime  $\gamma > 1$  can be seen as arising from the creation of a larger and larger set of equivalent edges (that scale linearly with  $T$ ). When the condensation phenomenon is strong enough (at some critical  $\gamma_c$ ), the models enter a no-recovery phase where all temporal information is lost. This threshold is certainly no greater than 2, because the star-like graphs of this regime—i.e., full condensates—are completely unorderable. If we are able to find positively correlated histories beyond  $\gamma = 2$  in Fig. 3, it is only because the system is small. Scale the network up and our predictive power vanishes, see Fig. 4.

While it is clear from the phenomenology of the generative model that the transition lies at some  $\gamma_c \leq 2$ , its exact location is harder to pinpoint. The difficulties stem from the fact that we can only inspect the transition through the lens of a good, but suboptimal algorithm (c.f. Sec. 2.9). Thus, even if the finite-size scaling analysis of Fig. 4 tells us that the OD fails at some  $\gamma_c^{\text{OD}}$ , it is possible that a better method will work until a true no-recovery threshold  $\gamma_c \geq \gamma_c^{\text{OD}}$  is reached. That being said, we can reach a number of conclusion from the imperfect analysis of Fig. 4. First, the figure tells us that, perhaps surprisingly,  $\gamma = 1$  is only special in that it marks the end of the regime where there are no obvious information sinks. Scalable inference appears possible well above the appearance of a condensate. Second, the figure suggests that the OD fails *discontinuously* at  $11/10 < \gamma_c^{\text{OD}} < 5/4$  in the network limit, because it achieves an average correlation that goes to zero with growing  $T$  above  $\gamma_c^{\text{OD}}$ , while it converges to an average correlation greater than 0 at  $\gamma_c^{\text{OD}}$ .

Whether an optimal algorithm will behave similarly remains an open question. Based on the effect of the condensate on the remainder of the network, we conjecture that  $\gamma_c$  is aligned with one of the transitions  $\gamma_m = (m+1)/m$  of the generative model, for  $m \leq 9$  (from Fig. 4). The most likely value is  $\gamma_c = 3/2$ , because the networks generated by the model change *drastically* at this point. Above  $\gamma = 3/2$ , they comprise of nodes of degree 2 or less that can—and do—cluster around a highly attractive central node (encoding next to no temporal information). Below  $\gamma = 3/2$ , the networks contains infinitely many nodes of degree 3 that must necessarily organize in large scale structures (that encode temporal information).

### 2.8.3 Nearly perfect inference

It is somewhat ironic that the overabundance of nodes of low degree leads to the onset of a no-recovery phase in the regime  $\gamma \gg 0$ , because these nodes have the exact opposite effect in the other extreme  $\gamma \ll 0$ . Indeed, in the presence of extreme homogeneity, the networks are effectively grown as a random path, where all nodes are of degree two or less (paralleling the regime  $\gamma \gg 0$ ). An important difference, however, is the edges are repulsive. For  $\gamma$  far enough from 0, this effect is so strong that the edges are added recursively to randomly chosen sides of the network, until a path of length  $T$  is obtained. The end result is always a path of length  $T$ , whose root is the  $k$ -th edge with probability  $\binom{T}{k}/2^T$ . Standard concentration inequalities tell us that the root will be close to the center with overwhelming probability in the limit of large  $T$ . Near perfect inference is then trivial: Peeling the path symmetrically from both sides yields a close approximation of the arrival time of every edge.

### 2.8.4 Effect of cycles

The above conclusions explicitly rely on the fact that the network are trees, i.e., that  $b = 1$ . It turns out, however, that many of these conclusions carry over to the case  $b < 1$ , as highlighted by the similarity of Figs. 3–4. There are essentially two areas where allowing for cycles brings notable differences: Near-perfect inference becomes impossible when  $\gamma \ll 0$ , and the correlation decreases much faster with growing  $\gamma$ .

The disappearance of the near perfect inference phase is imputable to long-range connections. Extreme homogeneity means that nodes of degree one (“leaves”) are almost always selected when two existing nodes must be connected; the resulting edges close dangling paths and erase all temporal information along these paths. Furthermore, if there are no available leaves, then a random and potentially long-range connection

is instead created, an even worse outcome for temporal inference. The net result is that the limit  $\gamma \rightarrow -\infty$  actually poses a hard challenge for any  $b < 1$ , mirroring the limit  $\gamma \rightarrow \infty$ . The near perfect inference phase is thus highly uncharacteristic of the general model.

If the correlation diminishes more abruptly when  $b < 1$ , it is because cycles, self-loops and parallel edges—all allowed motifs in the regime  $b < 1$ —accentuate the condensation phenomenon. A typical network realization in the super-linear regime  $\gamma > 1$  with  $b < 1$  comprises of: Many (unordered) self-loops centered on the condensates; a number of parallel edges connecting high degree nodes; and star-like node arrangements around high-degree nodes. The information sinks of the case  $b = 1$  are thus both larger and better interconnected. Furthermore, the topological constraints on the networks are weaker, because it is possible for nodes of degree greater than 2 to aggregate around a few attractive nodes, thanks to the self-loops, parallel edges, and cycles. Combining these two effects leads to a sharper decline of the correlation with growing  $\gamma > 1$ .

## 2.9 On the quality of the inference methods

Our numerical results suggest that even though the naive degree-based approach works relatively well in the regime  $\gamma > 0$ , the MMSE estimators and the onion decomposition actually perform much better across the board. This gap can be understood in terms of two simple requirements on accurate estimators. First—it is somewhat tautological, but worth stating explicitly—accurate estimators must return arrival times that are correlated with the ground-truth. Second, their discriminative power must grow with  $T$ —otherwise we run in the condensation problem anew. The case of the degree estimators on scale-free trees ( $\gamma = 1$  and  $b = 1$ ) is particularly illuminating in this regard. Scale-free networks contain infinitely many degree classes. This means that the degree estimators partition the edges in extremely fine classes. Yet they perform sub-optimally, because they fail on the first count: Degree classes are simply not very well correlated with the arrival times in this case, somewhat against our intuition [5]. Thus discriminative power alone is not enough; it must be accompanied by precise temporal information. But if it also vanishes, then the failure is complete (see, e.g., the degree estimators in the homogeneous regime).

If the onion decomposition and the MMSE estimators are so good, it is because they satisfy both criteria (correlation and discriminative power). Of these two methods, the correlation attained by the MMSE estimators is perhaps the least surprising; they after all build on an explicit knowledge of the growth model. In fact, we can write the average correlation of an inferred history  $Y$  as

$$\langle \rho(X, Y) \rangle \propto \rho(Y, Z) \tag{5}$$

where the average on the left-hand side is taken over  $P(X|G, \theta)$  and where  $Z$  is the MMSE history (see Supplementary Information for the derivation). Hence, anything short of using the MMSE estimators yields worst results on average, according to the posterior distribution.

The result that needs explaining, then, is the excellent average correlation achieved by the OD. Much like the degrees, the discriminative power of the OD grows with  $T$ , since the diameter of the networks grows with  $T$ . Different from the degrees, however, the quality of the age-correlation uncovered by the OD is far greater. Notice that the vast majority of histories  $X \in \Psi(G)$  place central edges at the beginning, and peripheral edges at the end [30, 46]. This is a simple consequence of the fact that there are many more consistent ways of enumerating the graph  $G$  starting from its center than from its periphery. The net result is that the MMSE estimators of the central edges are heavily skewed towards early arrival time, while that of the edges in the periphery are skewed towards later times (see Eq. (2)). Therefore, the separation in layers uncovered by the OD is actually contained directly in the posterior distribution—the onion decomposition is good *because* it approximates the optimal MMSE estimators.

It is important to note that the close connection between the OD and the MMSE estimators is valid on trees, but also on networks with cycles ( $b < 1$ ). Adding cycles does not alter the fact that the majority of

histories place peripheral edges towards the end; Their performances are similar even in the regime  $b < 1$  [see Fig. 3 (b)]. This is a most welcome observation, because the OD is far more efficient than sampling: The OD returns its *final* estimators in  $O(|E| \times \log |V|)$  steps [39], whereas a single *sample* is generated in roughly as many steps by the importance sampling algorithm. The above argument hence provides a justification for replacing complete sampling by the OD on any large networks, where sampling is impractical.

## 2.10 New insights on related analyses

At this point, we ought to discuss important connections with related work on root-finding [27–30] and complete history inference [33, 34], on random and preferential trees [i.e. for the models  $(\gamma, b) = (0, 1)$  and  $(1, 1)$ ]. These previous analyses establish optimal algorithms to find *node* orderings; so let us define the operator  $\tilde{\tau}_X(v)$ , identical to  $\tau_X(e)$  on vertices.

The most comprehensive root-finding method is put forward in Ref. [27]. Their strategy is to compute the number of histories  $\varphi(v) = |\{X | \tilde{\tau}_X(v) = 0\}|$  rooted on  $v$ , and to return the  $K$  nodes with the largest  $\varphi(v)$ . Of particular interest is the fact that they manage to bound the expected error rate  $\varepsilon$  in the cases  $\gamma = 0$  and  $\gamma = 1$ . It is shown that surprisingly, in both cases, this algorithm can find a set of size  $K(\varepsilon)$  independent of  $T$  and achieve a fixed error rate  $\varepsilon$ . Furthermore, it is shown that the case  $\gamma = 0$  is easier than the case  $\gamma = 1$  (smaller sets are needed to attain the same error rate  $\varepsilon$ ). Our results (Fig. 5) corroborates these observations and put them in the broader context of Bayesian inference with general  $\gamma$  (a generalization suggested in Ref. [27]). For example, notice that  $\varphi(v)$  is in fact proportional to the posterior probability

$$\varphi(v) \propto \sum_{X \in \Psi(X)} \mathbb{I}[\tilde{\tau}_X(v) = 0] P(X|G, \gamma) \equiv P[v \text{ is first} | G, \theta], \quad (6)$$

when the distribution  $P(X|G, \gamma)$  is uniform. Thus the estimators of Refs. [27, 28, 30] can be in fact seen as outputting the  $K$  first maxima of the marginal distribution for the first node of  $G$ , assuming a uniform posterior distribution<sup>1</sup>. The estimator appearing in Eq. (4) accounts for general parametrization, and point the way to obvious extensions to more complicated root graphs [29].

Another consequence of the generalization to arbitrary exponents  $\gamma$  is that we are able to establish the asymptotic behavior of optimal root-finding algorithms at the two extremes of the  $\gamma$  spectrum (again, defined in terms of node). As mentioned above, the networks are essentially star graphs in the regime  $\gamma \gg 0$ . Because all the nodes of a star-graph could have been part of the first edge; we expect a vanishing success rate of  $1 - \varepsilon = K/(T + 1)$  if  $\gamma \gg 0$ . In the strongly homogeneous regime, the model effectively generates randomly grown paths; given a chain (see discussion above), the optimal strategy is to predict that the  $K$  most central nodes are the most probable roots. The normal approximation of the binomial distribution tells us that that this set will actually contain the root with probability

$$1 - \varepsilon = \sum_{\ell=(T-K)/2}^{(T+K)/2} \frac{\binom{T}{\ell}}{2^T} \approx \int_{(T-K)/2}^{(T+K)/2} dx p(x) = \operatorname{erf} \left( \frac{K}{\sqrt{2T}} \right) \approx \sqrt{\frac{2}{\pi T}} K + O(T^{-3/2}), \quad (7)$$

where  $p(x)$  is the probability density function of the normal distribution of mean  $T/2$  and variance  $T/4$ . Therefore, to avoid an error rate  $\varepsilon$  that goes to 1 in the strongly homogeneous regime, the size of  $\mathcal{R}$  set must scale as  $T^{1/2}$ . This scaling is needed to tackle fluctuations in the generating mechanisms, rather than inherent weaknesses of the estimators; any smaller  $K(T)$  will yield error rates close to 1. And while the above discussion is phrased in terms of nodes (as in Ref. [28, 30, 46]), the scaling result also holds for root-finding problems defined in terms edges (one should output the  $T^{1/2}$  most central edges).

<sup>1</sup> $P(X|G, \gamma)$  in fact uniform when  $\gamma \in \{0, 1\}$ , due to an equivalence with random recursive trees [35]; the analysis of Refs. [27, 28] is therefore exact in these cases, as noted the authors.

Turning to related work on complete history recovery, we note that the recent analysis of Ref. [33] also relies on a peeling algorithm, almost isomorphic in its action to the onion decomposition [39]; it is shown in this reference that the algorithm performs extremely well on scale-free trees ( $\gamma = 1$  and  $b = 1$ ), in line with our analysis. Importantly, the notion of inference quality used in Ref. [33] is different from ours, because the authors point out the fact that there is a trade-off between precision and density (number of ordered pairs of nodes). In particular, when the peeling algorithm is allowed to withhold judgment on contentious pairs of nodes, one obtains nearly perfectly accurate estimates, at the cost of a small estimate density. Our analysis showcases another aspect of the power of peeling-type algorithms: They are also nearly optimal—i.e., as effective at extracting information as the best estimators—when all pairs must be ordered.

## 2.11 Generative modeling of real networks with random attachment

Preferential attachment—in its original form—only fits very few systems [50, 52], due to the fact that its statistical signature is extremely peculiar (a power-law degree distribution of exponent  $-3$ ). But as we now argue, our slight generalization suffices to turn it into a useful model of a number of real systems. First and most obviously, a parameterized attachment kernel drastically broadens the scope of application of the model [37]: With arbitrary attachment exponents, the model can fit exponential degree distributions ( $0 < \gamma < 1$ ), extremely heterogeneous distributions ( $\gamma > 1$ ), and homogeneous networks ( $\gamma < 0$ ). Allowing for cycles ( $b < 1$ ) broaden this scope even more. The good fit of the degree distribution of a real network not drawn from the model is an unmistakable sign of this flexibility (see caption of Fig. 6). Second, random attachment (with  $b = 1$ ) is very specific in its prescription, because nodes can never actively generate new edges after they have joined the network. This is obviously uncharacteristic of many systems. Hence, there are also *temporal* reasons underpinning the necessity of a more general model: A ratio  $b = |V|/|E|$  far from unity can be seen as evidence for the fact that connections occur beyond the initial attachment events [40]. Whether this is appropriate will, of course, depend on the specifics of the investigated systems.

With this in mind, our generalization of PA makes sense as a model for the email network investigated in the result section (see Fig. 6). New individuals joining the network must necessarily attach *somewhere*—a phenomenon that we model through the initial edge of every node. Edges do appear after this initial event—which we model with  $b < 1$ .

The estimated parameters are consistent with the fact that the email network is overlaid on a social system. First, attachment is far from preferential (with an estimated kernel exponent of  $\hat{\gamma} \approx 0.07$ ). This is in line with the observation that social capacities are limited, as famously argued in the anthropological theory known as Dunbar’s number [53, 54]. The degree distribution cannot be too skewed, because there are constraints on the maximal number of connections that can be entertained simultaneously by any given individual. Second, the estimated ratio  $\hat{b} \approx 0.62$  signals that existing nodes share many edges—the network, while sparse, is definitely not a tree. This can be seen as a consequence of the fact that social networks are dense webs of connections, most of which are not formed at attachment (they are instead formed later through, e.g., triadic closure [55]). Therefore,  $b < 1$  is needed to capture the structural signature of a socially driven growth.

Beyond the conclusive test of goodness-of-fit for the degree distribution, another reliable indicator that the model is suitable for the investigated system is the ordering of the inference results. Paralleling the results on artificial networks in the heterogeneous regime  $\gamma = 0.07$ , we find that the MMSE estimators are the best, but they are closely followed by OD, with the degrees behind. This tells us that temporal information is encoded in the network in a way that is consistent with the generative model.

## 2.12 Looking ahead: challenges and generalizations

The opportunities brought about by network archaeology are tantalizing; in bioinformatics alone—the only field where it has found widespread adoption thus far—, network archaeology with the divergence-duplication models has already yielded insights into the past states of real PPI networks [16, 19] and, e.g., improved on network alignment [17, 18]. Generalization to models that are relevant to social and technological networks will allow us to answer new questions about the past of static systems, and to improve on network analysis techniques [56].

The present paper provides a simple framework to carry this program forward. With a model specified as a Markov chain, importance sampling provides weighted histories that can be aggregated with MMSE estimator to yield optimal estimators of the true history of a network. Different models will require different proposal distributions  $Q(X)$ , but the prescription is almost automatic. Drawing from a background network will always work, as long as histories leave tangible traces (i.e., there are no deletion events [20]).

That being said, our analysis is of course not complete, and leaves a number of important theoretical and computational problems open. First, while we have provided compelling evidence for the existence of a scalable inference and no-recovery phases (in the general model  $b \leq 1$ ), we have not pinpointed the location  $\gamma_c(b)$  of the transition that separates them; our analysis suggest that it lies at some rational value  $\gamma_c = (m + 1)/m$  for  $m \leq 9$  (probably at  $\gamma_c = 3/2$  when  $b = 1$ .) Second, we have shown that the root-finding on trees goes from hard ( $\gamma \rightarrow -\infty$ ), to easy ( $\gamma = 0$  and  $\gamma = 1$ ), to impossible ( $\gamma \gg 0$ ) as  $\gamma$  is varied. Our numerical evidences suggest that there exists a point  $\gamma < 0$  where root-finding is even easier than at  $\gamma = 0$ ; whether this point can be found remains an interesting challenge. Third, we have shown that the MMSE estimators are optimal in the sense that they maximize the correlation averaged over the posterior distribution (see Eq. (5)). This begs the question: do they also satisfy other notions of optimality? And can we prove that they have other interesting properties, and in particular that they are guaranteed to be consistent with  $G$ ? We conjecture that the latter is true (we have found no counter-examples). Finally, we have argued for using the OD [39] / peeling algorithm [33] in large networks because importance sampling is not scalable, at least not for the purpose of network archaeology. This substitution will most likely not work with different models, because it is based on a close correspondence between the posterior averages of arrival times, and the order of peeling of a network. As a result, the next step—and the most important open problem in our opinion—will be to derive efficient approximations methods that work with general models, to allow for flexible network archaeology. These methods will have to handle models specified as chains  $P(X|\theta)$  with some arbitrary notion of consistency  $P(G|X, \theta)$ . The relaxation technique of Ref. [57] for permutation inference comes to mind; but also dynamical variants of message-passing [58], perhaps in the spirit of Ref. [59].

## 3 Materials and Methods

### 3.1 Generative model

We consider a generative model that generalizes the classical preferential attachment model (PA) of Barabási-Albert [5]. The salient features of the generalization are a non-linear attachment kernel  $k^\gamma$  [37] and the possibility for new links to connect pairs of existing nodes (see Refs. [36, 38, 40, 41] for related models).

This model generates sequences of undirected graphs  $G_0, \dots, G_{T-1}$ , where  $G_{t-1}$  has one fewer edge than  $G_t$ . We summarize a particular sequence of graphs using the *history* of the generative process, i.e., a tuple  $X = (e_0, \dots, e_{T-1})$ , where  $e_t$  is the edge added to the sequence at time step  $t$ .

Random growth events are resolved as follows. At time step  $t$ , we first draw a random node from  $V_t$ , the node set of  $G_t$  prior to any modifications of the graph's structure. Node  $i$  is selected with probability

$$w_i(\gamma, G_t) = \frac{k_i^\gamma(t)}{\sum_{j \in V_t} k_j^\gamma(t)}, \quad (8)$$

where  $\gamma \in \mathbb{R}$  is the attachment kernel, and where  $k_i(t)$  is the degree of node  $i$  at time  $t$ , *before* the new edge is added. We then complete the edge with a *new* node with probability  $b$ , and with an existing node with complementary probability  $1 - b$  (a *densification* event). When densification events occur, the second is selected randomly with weights given by Eq. (8). In principle, these events may lead to parallel edges and self-loops, which we allow for simplicity. However, the number of redundant edges and self-loops is vanishing for all  $b$  in the large networks limit, for any kernel  $\gamma$  smaller than 1 (see Supplementary Information).

This model corresponds to an out of equilibrium Markov process, fully specified by one-step transition probabilities. It induces a distribution  $P(X|\gamma, b)$  on all possible histories of length  $T$  that can be written as a simple product. Denote by  $e_t = (e_t(1), e_t(2))$  the  $t$ -th edge in  $X$ , and let  $\mathbb{I}_X(t)$  be an indicator variable that is equal to 1 if  $e_t$  contains a node not previously seen in  $X$  (set it to 0 otherwise). Furthermore, construct the edges such that  $e_t(2)$  is always the new node, whenever there is one. Then we have

$$P(X|\gamma, b) = \prod_{t=1}^{T-1} w_{e_t(1)}(\gamma, G_t) \left\{ \mathbb{I}_X(t)b + [1 - \mathbb{I}_X(t)](1 - b)w_{e_t(2)}(\gamma, G_t) \right\}. \quad (9)$$

The posterior probability  $P(X|G, \gamma, b)$  is obtained by conditioning on a labeled graph  $G$ . To do so, we first define the *consistency* of a history  $X$  with a graph  $G$ , denoted  $X \Rightarrow G$ . A history  $X$  is said to be consistent with  $G$  if the labeled graph  $G'$  with edge set  $\{e|e \in X\}$  is isomorphic to  $G$ , and  $P(X|\gamma, b) > 0$ . It is easy to see that there are many different histories consistent with  $G$ , but that there is only one labeled graph  $G'$  associated with each  $X$  (there is a surjection of history onto graphs). Therefore, the probability  $P(G|X, \gamma, b) = 1$  if and only if  $X$  is consistent with  $G$ , and it is normalized. Bayes formula allows us to write

$$P(X|G, \gamma, b) = \frac{P(X|\gamma, b)}{P(G|\gamma, b)} \mathbb{I}[X \Rightarrow G], \quad (10)$$

where  $\mathbb{I}[S]$  is the indicator function, equal to 1 if the statement  $S$  is true, and to 0 otherwise. Although not directly useful for estimation purposes, the probability  $P(G|\gamma, b)$  is in principle defined. It is obtained by summation:

$$P(G|\gamma, b) = \sum_{X \in \Phi_T} P(X|\gamma, b) P(G|X, \gamma, b) = \sum_{X \in \Psi(G)} P(X|\gamma, b), \quad (11)$$

where  $\Phi_T$  is the set of all histories of length  $T$ , and where  $\Psi(G) \subseteq \Phi_T$  is the set of histories consistent with  $G$ .

### 3.2 Inference task

Let  $\tau_X(e) \in \{0, \dots, T-1\}$  denote the position of edge  $e$  in history  $X$  (also called its arrival time). Our goal is to give the best possible estimate of  $\{\tau_{\tilde{X}}(e)\}_{e \in G}$  for the labeled graph  $G$ , where  $\tilde{X}$  is the real history of

$G$  (the ground-truth). By convention, we express both the estimators and the true history in the time scale  $t = 0, \dots, T - 1$  where  $T = |E|$ . Note, however, that the estimator  $\hat{\tau}(e)$  of  $\tau_{\hat{X}}(e)$  need not be an integer or distinct for other estimators [i.e., we allow  $\hat{\tau}(e) = \hat{\tau}(e')$ ].

We quantify the quality of the estimators  $\{\hat{\tau}(e)\}$  of the true arrival times using the Pearson product-moment correlation coefficient

$$\rho = \frac{\sum_{e \in E(G)} (\tau_{\hat{X}}(e) - \langle \tau \rangle)(\hat{\tau}(e) - \langle \tau \rangle)}{\sqrt{\sum_{e \in E(G)} (\tau_{\hat{X}}(e) - \langle \tau \rangle)^2} \sqrt{\sum_{e \in E(G)} (\hat{\tau}(e) - \langle \tau \rangle)^2}}, \quad (12)$$

where  $\langle \tau \rangle = (T - 1)/2$ , and where we have dropped the subscript for the sake of conciseness. In taking the sum, it is assumed that the edges are distinguishable (this matters for multigraphs with self-loops). The Pearson product-moment correlation has a few useful properties adapted to the network archaeology problem. One, it is not affected by an arbitrary linear transformation of the timescales; this captures the fact that the timescales of the compared histories are in fact arbitrary. Two, it penalizes spurious ordering of events; if a graph contains no information on the ordering of a subset  $S \subseteq E$  of the edges, creating a random ordering of the edges in  $S$  yields a worst outcome on average than attributing the average time of arrival  $\lambda$  of all edges in  $S$ , to all edges in  $S$  (see Supplementary Information). Three, it has clear bounds; it takes values in  $[-1, 1]$ , where  $|\rho| = 1$  indicates a perfect recovery up to a time-reversal, and where  $|\rho| = 0$  indicates that no information is extracted from the graph at all (e.g., when the ordering is completely random, or all edges are declared tied). Thus the Pearson product-moment correlation captures both aspects of the recall measures introduced in Ref. [33]: It penalizes low-density estimator (i.e., estimators that declare too many ties), and reward accurate orderings.

### 3.3 Topological estimation algorithms

We regroup in this category the methods that rely only on the structure of  $G$  to make predictions, forgoing explicit knowledge of the posterior distribution  $P(X|G, \theta)$ . These methods all follow the same formula: We first rank the edges, based on some network property (degree, centrality, etc.), and then output these ranks as  $\{\hat{\tau}(e)\}$ , the estimated arrival times. Whenever the edges of a subset  $S \subseteq E$  are indistinguishable, we give them the same rank  $\lambda(S)$ , reflecting our uncertainty of their true ordering. We chose a  $\lambda(S)$  that preserves the overall average time of arrival  $\langle \tau \rangle$ ; this yields  $\lambda = t + (m + 1)/2$ , where  $m = |S|$  and  $t + 1, \dots, t + m$  are the ranks that would have been assigned to the edges of  $S$ , had they been ordered. This choice is optimal in the sense that assigning any other rank to the edges of  $S$  would not reliably increase the overall correlation (see Supplementary Information). Furthermore, it has the added benefit that the Pearson correlation can then be computed directly as Spearman’s rank correlation, if one considers the arrival time as the rank.

#### 3.3.1 Degree-based estimation

For all parametrization of the generative model, nodes that arrive earlier in the process have, on average, a larger degree [5, 37, 45, 60]. We use the degree of nodes to induce a ranking of edges as follows. Let  $(k_e^{\text{low}}, k_e^{\text{high}})$  denote the degree of the nodes connected by edge  $e$ , with  $k_e^{\text{low}} \leq k_e^{\text{high}}$ . We rank edges in descending order with  $k_e^{\text{high}}$ , and break ties with  $k_e^{\text{low}}$ , when possible. The equalities that remain are declared as such. We then use the rank as the estimated time of arrival, with the tie-break rule highlighted above.

#### 3.3.2 Layer-based estimation

The onion decomposition (OD) generalizes the  $k$ -core decomposition. The method is based on the classical  $O(|E| \times \log |V|)$  algorithm for the  $k$ -core decomposition [39, 48]: it peels networks by iteratively removing all nodes, starting from the lowest degree nodes. A  $k$ -shell comprises all nodes that can be removed by iteratively removing nodes of degree  $k$  or less. Different from the classical algorithm, the OD treats each batch of removal as a separate layer; this assigns both a coreness and a layer number to each node. We

assume that nodes in the lowest  $k$ -shells appeared last and that, within a shell, the first node to be removed is the last to have entered. A simple modification allows the algorithm to order the *edges*: An edge is assigned to a pass as soon as one of its nodes is peeled away. All edges removed in the same pass are declared as tied. Because we effectively discard the coreness number to order edges and nodes, the OD is almost equivalent to the peeling algorithm of Ref. [33], that proceeds by iteratively removing the lowest degree nodes. The only difference is that nodes of low but different degrees are sometimes removed simultaneously in the OD [39].

### 3.4 Sampling algorithms

A principled estimation of  $\tau(e)$  must rely on the posterior distribution  $P(X|G, \gamma, b)$ . We use the minimum mean square error (MMSE) estimator of  $\tau(e)$ , given by

$$\hat{\tau}(e) = \langle \tau_X(e) \rangle_{P(X|G, \gamma, b)} = \sum_{X \in \Psi(G)} \tau_X(e) P(X|G, \gamma, b), \quad (13)$$

since it maximizes expectation of the correlation a posteriori (see Supplementary Information). We also note that it is more robust than the other natural alternative, namely the mean maximum overlap (MMO) estimator, obtained by finding the time  $t$  that maximizes the marginal posterior probability  $p_t(e) = \sum \mathbb{I}[\tau_X(e) = t] P(X|G, \gamma, b)$  over all  $t$ . Indeed, the maximum of  $p_t(e)$  with respect to  $t$  is frequently not unique, because many pairs of edges are truly unorderable [33]. In the presence of the slightest perturbation, these equivalence classes collapse (or must be diagnosed using a costly post-processing step), leading to poor performances of the MMO estimator. In contrast, the MMSE estimators hardly changes when the empirical estimation of  $p_t(e)$  is inexact, leading to robust predictions.

The support of the posterior distribution is far too large to handle analytically. This forces us to resort to sampling methods, and approximate  $\hat{\tau}(e)$  as

$$\hat{\tau}(e) \approx \frac{1}{n} \sum_{i=1}^n \tau_{x_i}(e), \quad (14)$$

where  $x_i$  is a random history of length  $T$  drawn from the posterior distribution.

In practice it is hard to sample from  $P(X|G, \gamma, b)$ , and we will prefer a transformation of Eq. (13). Given an easy-to-sample stochastic process that enumerates the edges of  $G$  with probability  $Q(X|G)$ , we express the MMSE estimator of  $\tau(e)$  as

$$\begin{aligned} \hat{\tau}(e) &= \sum_{X \in \Psi(G)} \frac{\tau_X(e) P(X|\gamma, b) Q(X|G)}{P(G|\gamma, b) Q(X|G)} \\ &= \frac{\langle \tau_X(e) \omega(X|G, \gamma, b) \rangle_{Q(X|G)}}{P(G|\gamma, b)}, \end{aligned} \quad (15)$$

where  $\omega(X|G, \gamma, b) = P(X|\gamma, b)/Q(X|G)$  is the sample weight. Equation (15) is then well approximated by

$$\hat{\tau}(e) \approx \frac{1}{nP(G|\gamma, b)} \sum_{i=1}^n \tau_{x_i}(e) \omega(x_i|G, \gamma, b), \quad \text{where } \{x_i\} \stackrel{i.i.d.}{\sim} Q, \quad (16)$$

in the large  $n$  limit. But different from Eq. (14), this second formulation has a control parameter—the *proposal distribution*  $Q(X|G)$ —that can be used to simplify the sampling process and/or enhance convergence. This re-weighting scheme is known as the importance sampling method [61].

In modifying the expression for the estimator, we have introduced an intractable normalization  $P(G|\gamma, b)$ . This issue can be side-stepped by noticing that the estimators  $\langle \tau(e) \rangle$  must satisfy the sum

$$\begin{aligned} \sum_{e \in E(G)} \langle \tau(e) \rangle &= \sum_{e \in E(G)} \sum_{X \in \Psi(G)} \tau_X(e) P(X|G, \gamma, b) \\ &= \sum_{X \in \Psi(G)} P(X|G, \gamma, b) \sum_{e \in E(G)} \tau_X(e) = \binom{T}{2}, \end{aligned} \quad (17)$$

where the last equality follows from the normalization of  $P(X|G, \gamma, b)$ . Thus we compute  $\hat{\tau}(e)$  up to a multiplicative constant and use Eq. (17) to set the scale of the estimators.

### 3.4.1 Variance reduction

One of the advantages of the importance sampling method is that the proposal distribution  $Q(X|G)$  can be used to explicitly control the variance of the estimators. The lower this variance, the better, since fewer samples are then needed to evaluate the estimators accurately [61].

In our case, the variances of interest are those associated with the MMSE estimators of Eq. (16). Minimizing these variances separately is however not useful, because the best sampling strategy—to update the complete set of estimators with every sample—relies on a single proposal distribution  $Q(X|G)$  shared by all the estimators. Thus, we ought not to minimize variances in isolation, but the sum of variances  $\sum \sigma^2(e)$ , where  $\sigma^2(e)$  is the variance of  $\tau_X(e)\omega(X|G, \gamma, b)$  for  $X$  drawn from  $Q(X|G)$ . Because the expectation  $\langle \tau_X(e)\omega(X|G, \gamma, b) \rangle_Q$  is actually independent from  $Q(X|G)$ , we may equivalently minimize the sum of second moments

$$\sum_{e \in E(G)} \sum_{X \in \Psi(G)} \tau_X^2(e)\omega^2(X|G, \gamma, b)Q(X|G) \propto \sum_{X \in \Psi(G)} \frac{P^2(X|G, \gamma, b)}{Q(X|G)}, \quad (18)$$

to the same effect.

It is easy to verify that  $Q(X|G) = P(X|G, \gamma, b) \forall X \in \Psi(G)$  is the optimum of Eq. (18), i.e., that the sum of the variances is the smallest when the proposal distribution is the target distribution  $P(X|G, \gamma, b)$ . This ideal proposal distribution is not easy to construct in general, but it can guide our choice of  $Q(X|G)$ : It tells us that we should try to mimic the generative process whilst generating a history  $X \Rightarrow G$ . We therefore introduce a simple alternative proposal distribution, with the aim of approximating  $P(X|G, \gamma, b)$ : The snowball sampling method.

### 3.4.2 Snowball sampling

A snowball sample is a random recursive enumeration of a graph, rooted at randomly selected seed [44, 62, 63]. More explicitly, given a random initial edge  $e_0$  (the seed), define the *boundary* as the set of all non-enumerated edges that share at least one node with  $e_0$ . Then select an edge  $e_1$  from the boundary uniformly at random, and update the boundary by adding all new edges reached with  $e_1$ , repeating the process for  $e_2, e_3, \dots$ , until the graph is exhausted. Because this algorithm draws the edge from the observed graph  $G$  (the “background graph” [46]), it generates a history  $X$  that is necessarily consistent with  $G$ . Thus, the algorithm is efficient in the sense that it (a) always generates a plausible history without rejection, and (b) has a polynomial worst-time complexity of  $O(|E| \times k_{\max})$ , where  $k_{\max}$  is the maximal degree.

The probability of generating a history  $X$  with the snowball sampling algorithm is given by

$$Q_{\text{sb}}(X|G) = P(e_0|G) \times \prod_{t=1}^{T-1} [|\Omega_X(t)|]^{-1}, \quad (19)$$

where  $\Omega_X(t)$  denotes the boundary at step  $t$  of history  $X$ , and where  $P(e_0|G)$  is the distribution used to select the seed  $e_0$ . To bias the proposal distribution towards histories that begin with edges attached to high-degree nodes, we select the initial edge with probability proportional to  $(k_1 \times k_2)^\alpha$ , where  $\alpha$  is a parameter, and where  $(k_1, k_2)$  are the degrees of the nodes connected by an edge. This better mimics the ground truth and leads to a faster convergence of the estimators. Because the histories  $X$  are constructed iteratively, the resulting sampling method is called a *sequential importance sampling algorithm* [42].

### 3.4.3 Numerical stability

Since we cannot always achieve a proposal distribution close to the posterior distribution  $P(X|G, \gamma, b)$  the weights  $\omega(X_i|G, \gamma, b)$  of the samples  $X_i$  are not necessarily balanced. This can lead to severe numerical problems, which we avoid by adding a preliminary estimation step.

Using  $n_s \ll n$  i.i.d. samples drawn from  $Q$ , we first compute the empirical averages

$$\langle \mathcal{L}_P \rangle = \frac{1}{n_s} \sum_{i=1}^{n_s} \log P(X_i|\gamma, b) \quad \langle \mathcal{L}_Q \rangle = \frac{1}{n_s} \sum_{i=1}^{n_s} \log Q(X_i|G) . \quad (20)$$

We then split the sample weights and express the estimators of Eq. (16) as

$$\hat{\tau}(e) = \frac{\exp[\langle \mathcal{L}_P \rangle - \langle \mathcal{L}_Q \rangle]}{nP(G|\gamma, b)} \sum_{i=1}^n \exp[\Delta_P(X_i) - \Delta_Q(X_i)] \tau_{X_i}(e) , \quad (21)$$

where  $\Delta_P(X_i) = \log P(X_i|\gamma, b) - \langle \mathcal{L}_P \rangle$  and  $\Delta_Q(X_i) = \log Q(X_i|G) - \langle \mathcal{L}_Q \rangle$ . When the probabilities are tightly peaked about their expectations, both  $\Delta_P(X_i)$  and  $\Delta_Q(X_i)$  are small, and the sum becomes numerically stable. Again, the leading terms can be dropped since the estimators must satisfy the constraint appearing in Eq. (17).

### 3.5 Parameters estimation

In writing the sampling methods, we have conditioned the estimators  $\{\hat{\tau}(e)\}$  on  $(\gamma, b)$ , because as we now show, the parameters can be estimated from a single, static, observed network  $G$ .

The ratio of the number of nodes to the number of edges is an obvious estimator for  $b$ , i.e.,

$$\hat{b}(G) = \frac{|V(G)| - 2}{|E(G)| - 1} . \quad (22)$$

This is due to the fact that the observed graph can be seen as a signature of  $|E| - 1$  i.i.d. Bernoulli trials of parameter  $b$ . Each edge beyond the first embodies a test of whether a new node should be added, and each node beyond the two initial nodes signals a success of the trial.

The exponent  $\gamma$  poses a harder challenge. Direct estimation involves a complex a posteriori estimate of  $P(\gamma|G, b) \propto P(\gamma|b) \sum_X P(X|\gamma, b)$ , where  $P(\gamma|b)$  is a Bayesian prior on  $\gamma$ . Neither maximizing this posterior distribution nor evaluating its average is easy, since both approaches require the calculation of an intractable sum (where  $\gamma$  appears as a continuous exponent). In particular, this prevents the use of known estimation methods based on time-resolved graphs [13, 15, 64], because too many estimates would have to be combined.

We instead opt for a simpler solution based on the degree distribution, namely the now standard Kolmogorov-Smirnov (KS) minimization approach of Ref. [50]. The KS-statistic of a pair of noisy distributions  $(P, Q)$  is given by the supremum of the difference of their cumulative distribution function (CDF), i.e.,

$$D(P, Q) = \sup_k |f_P(k) - f_Q(k)| , \quad (23)$$

where  $f_P(k)$  is the CDF of  $P$  at point  $k$ . Given an empirical degree distribution  $P(G)$  derived from an observed network  $G$ , we learn  $\gamma$  by minimizing the KS-statistic averaged over  $n$  random degree distributions  $\{Q^{(i)}(\gamma)\}_{i=1, \dots, n}$  generated by the model of parameters  $(\gamma, \hat{b})$ . The minimum  $D^*(G)$  can be found efficiently using Brent's method [65], since the average KS-statistic is convex. We use  $n \gg 1$  random instances to compute  $D$  at each evaluation, to ensure that the resulting function is smooth enough for the optimizer to converge to its true minimum. When  $T$  is large, generating  $n \gg 1$  networks can be costly, because a simulation runs in  $O(T^2)$  time. Therefore, in practice, we instead first compute the expected degree distribution of the model using mean-field equations, and then draw  $n$  finite samples from the resulting distribution. This approach is equivalent to—but much faster than—direct simulations.

We note in closing that the above framework provides a natural notion of goodness-of-fit for  $\gamma$  [50]. Indeed, the goodness-of-fit can be assessed by first generating few random degree distribution with the estimated parameters  $(\hat{\gamma}, \hat{b})$ , and then applying the complete testing procedure anew, using the random degree distributions as the reference empirical distributions. This provides a null distribution for  $D$ , which tells us whether  $D^*(G)$  is an extreme value of the average KS-statistic or not. Following the standard, we assume that if  $P[D > D^*(G)] > 0.1$ , then the fit is good [50].

### 3.6 Experimental pipeline

In all numerical experiments, we randomize both the node labels and the order in which the edge list is passed to the algorithms, as to hide any implicit temporal information contained in the tags of the nodes and ordering of the edges. All posterior averages are evaluated with the true parametrization of the model, when the networks are artificial (Fig. 3 and 5). The parameters are estimated in experiments involving real networks.

### 3.7 email-Eu-core dataset

The datasets analyzed in the Result and Discussion sections consists of a series of anonymized emails, sent within a large European research institution [49]. It comprises 332 334 emails sent between 986 individuals, over a span of 803 days. To construct a single undirected growing network from a series of emails (directed edges), we consider that two individuals become connected as soon as they have both sent  $n_c = 40$  emails to the other party. This filtration removes noise (e.g. institutional spam) and spurious interactions (e.g. transient contact) from the dataset. Our choice of threshold is motivated by the fact that the resulting network is not too small, yet sparse enough to be well-modeled by the  $(\gamma, b)$  generalization of PA. The results are robust to small changes in  $n_c$ , see Supplementary Information. We focus on the final giant component of the resulting network (294 nodes and 406 edges). To construct its history, we start from the end of the growth process, and out the largest component. We then run its history—the sequence of new edges—backward. When it absorbs smaller components (i.e., when more than one edge is removed from the component simultaneously in its reversed history), we consider that their edges appeared sequentially, as if they had been created at the time of the absorption.

### 3.8 Software

Implementations of the generative models and inference methods are available online at [github.com/jg-you/network\\_archaeology](https://github.com/jg-you/network_archaeology).

## Acknowledgments

This work was supported by the Fonds de recherche du Québec-Nature et technologies (JGY, EL, PD), the Conseil de recherches en sciences naturelles et en génie du Canada (GSO), the James S. McDonnell Foundation Postdoctoral Fellowship (LHD), the Santa Fe Institute (LHD), Grant No. DMS-1622390 from the National Science Foundation (LHD), and the program Sentinel North, financed by the Canada First Research Excellence Fund (JGY, EL, CM, GSO, PD). The authors also acknowledge the generous financial contribution of the AELIES. We thank Compute Canada and Calcul Québec for their infrastructure.

## References

- [1] L. Hébert-Dufresne, A. Allard, J.-G. Young, and L. J. Dubé, “Constrained growth of complex scale-independent systems,” *Phys. Rev. E*, vol. 93, no. 3, p. 032304, 2016.
- [2] G. St-Onge, J.-G. Young, E. Laurence, C. Murphy, and L. J. Dubé, “Phase transition of the susceptible-infected-susceptible dynamics on time-varying configuration model networks,” *Phys. Rev. E*, vol. 97, no. 2, p. 022305, 2018.
- [3] D. S. Callaway, M. E. J. Newman, S. H. Strogatz, and D. J. Watts, “Network robustness and fragility: percolation on random graphs,” *Phys. Rev. Lett.*, vol. 85, no. 25, p. 5468, 2000.
- [4] C. Castellano and R. Pastor-Satorras, “Relating topological determinants of complex networks to their spectral properties: Structural and dynamical effects,” *Phys. Rev. X*, vol. 7, no. 4, p. 041024, 2017.

- [5] A.-L. Barabási and R. Albert, “Emergence of scaling in random networks,” *Science*, vol. 286, no. 5439, pp. 509–512, 1999.
- [6] S. Thurner, R. Hanel, B. Liu, and B. Corominas-Murtra, “Understanding Zipf’s law of word frequencies through sample-space collapse in sentence formation,” *J. R. Soc. Interface*, vol. 12, p. 20150330, 2016.
- [7] G. Bianconi and A.-L. Barabási, “Bose-Einstein condensation in complex networks,” *Phys. Rev. Lett.*, vol. 86, no. 24, p. 5632, 2001.
- [8] H. A. Simon, *Models of Man; Social and Rational*. Wiley, 1957.
- [9] M. Mitchell, *Complexity: A Guided Tour*. Oxford University Press, 2009.
- [10] L. Hébert-Dufresne, A. Allard, V. Marceau, P.-A. Noël, and L. J. Dubé, “Structural preferential attachment: stochastic process for the growth of scale-free, modular, and self-similar systems,” *Phys. Rev. E*, vol. 85, no. 2, p. 026108, 2012.
- [11] L. Hébert-Dufresne, E. Laurence, A. Allard, J.-G. Young, and L. J. Dubé, “Complex networks as an emerging property of hierarchical preferential attachment,” *Phys. Rev. E*, vol. 92, no. 6, p. 062809, 2015.
- [12] J. Leskovec, L. Backstrom, R. Kumar, and A. Tomkins, “Microscopic evolution of social networks,” in *Proceedings of the 14th ACM SIGKDD International Conference on Knowledge discovery and Data Mining*, pp. 462–470, ACM, 2008.
- [13] V. Gómez, H. J. Kappen, and A. Kaltenbrunner, “Modeling the structure and evolution of discussion cascades,” in *Proceedings of the 22nd ACM conference on Hypertext and hypermedia*, pp. 181–190, ACM, 2011.
- [14] A. Z. Jacobs and A. Clauset, “A unified view of generative models for networks: models, methods, opportunities, and challenges,” *arXiv:1411.4070*, 2014.
- [15] T. Pham, P. Sheridan, and H. Shimodaira, “Joint estimation of preferential attachment and node fitness in growing complex networks,” *Sci. Rep.*, vol. 6, 2016.
- [16] S. Navlakha and C. Kingsford, “Network archaeology: uncovering ancient networks from present-day interactions,” *PLoS Comput. Biol.*, vol. 7, no. 4, p. e1001119, 2011.
- [17] J. Flannick, A. Novak, B. S. Srinivasan, H. H. McAdams, and S. Batzoglou, “Graemlin: general and robust alignment of multiple large interaction networks,” *Genome Res.*, vol. 16, no. 9, pp. 1169–1181, 2006.
- [18] J. Dutkowski and J. Tiuryn, “Identification of functional modules from conserved ancestral protein–protein interactions,” *Bioinformatics*, vol. 23, no. 13, pp. i149–i158, 2007.
- [19] J. W. Pinney, G. D. Amoutzias, M. Rattray, and D. L. Robertson, “Reconstruction of ancestral protein interaction networks for the bZIP transcription factors,” *Proc. Natl. Acad. Sci. U.S.A.*, vol. 104, no. 51, pp. 20449–20453, 2007.
- [20] R. Patro, E. Sefer, J. Malin, G. Marçais, S. Navlakha, and C. Kingsford, “Parsimonious reconstruction of network evolution,” *Algorithm Mol. Biol.*, vol. 7, no. 1, p. 25, 2012.
- [21] R. Patro and C. Kingsford, “Predicting protein interactions via parsimonious network history inference,” *Bioinformatics*, vol. 29, no. 13, pp. i237–i246, 2013.
- [22] S. Li, K. Choi, T. Wu, and L. Zhang, “Reconstruction of network evolutionary history from extant network topology and duplication history,” in *Proceedings of the 2012 International Symposium on Bioinformatics Research and Applications*, pp. 165–176, Springer, 2012.
- [23] S. Li, K. P. Choi, T. Wu, and L. Zhang, “Maximum likelihood inference of the evolutionary history of a ppi network from the duplication history of its proteins,” *IEEE T. Comput. Biol. Bioinformat.*, vol. 10, no. 6, pp. 1412–1421, 2013.
- [24] T. A. Gibson and D. S. Goldberg, “Reverse engineering the evolution of protein interaction networks,” in *Biocomputing*, pp. 190–202, World Scientific, 2009.
- [25] X. Zhang and B. M. E. Moret, “Refining transcriptional regulatory networks using network evolutionary

- models and gene histories,” *Algorithm Mol. Biol.*, vol. 5, no. 1, p. 1, 2010.
- [26] A. Jasra, A. Persing, A. Beskos, K. Heine, and M. De Iorio, “Bayesian inference for duplication–mutation with complementarity network models,” *J. Comput. Biol.*, vol. 22, no. 11, pp. 1025–1033, 2015.
- [27] S. Bubeck, L. Devroye, and G. Lugosi, “Finding Adam in random growing trees,” *Random Struct. Algor.*, vol. 50, no. 2, pp. 158–172, 2017.
- [28] M. Z. Rácz, S. Bubeck, *et al.*, “Basic models and questions in statistical network analysis,” *Stat. Surv.*, vol. 11, pp. 1–47, 2017.
- [29] G. Lugosi and A. S. Pereira, “Finding the seed of uniform attachment trees,” *arXiv:1801.01816*, 2018.
- [30] D. Shah and T. Zaman, “Rumors in a network: who’s the culprit?,” *IEEE T. Inform. Theory*, vol. 57, no. 8, pp. 5163–5181, 2011.
- [31] S. Mahantesh, S. Iyengar, M. Vijesh, S. R. Nayak, and N. Shenoy, “Prediction of arrival of nodes in a scale free network,” in *Proceedings of the 2012 International Conference on Advances in Social Networks Analysis and Mining (ASONAM 2012)*, pp. 517–521, IEEE Computer Society, 2012.
- [32] G.-M. Zhu, H. Yang, R. Yang, J. Ren, B. Li, and Y.-C. Lai, “Uncovering evolutionary ages of nodes in complex networks,” *Eur. Phys. J. B*, vol. 85, no. 3, p. 106, 2012.
- [33] A. Magner, A. Grama, J. K. Sreedharan, and W. Szpankowski, “Times: temporal information maximally extracted from structure,” 2017.
- [34] A. Magner, A. Grama, J. Sreedharan, and W. Szpankowski, “Recovery of vertex orderings in dynamic graphs,” in *Proceedings of the 2017 IEEE International Symposium on Information Theory (ISIT)*, pp. 1563–1567, IEEE, 2017.
- [35] M. Drmota, *Random trees: an interplay between combinatorics and probability*. Springer, 2009.
- [36] T. Pham, P. Sheridan, and H. Shimodaira, “PAFit: a statistical method for measuring preferential attachment in temporal complex networks,” *PLoS ONE*, vol. 10, no. 9, p. e0137796, 2015.
- [37] P. L. Krapivsky, S. Redner, and F. Leyvraz, “Connectivity of growing random networks,” *Phys. Rev. Lett.*, vol. 85, no. 21, p. 4629, 2000.
- [38] R. Albert and A.-L. Barabási, “Topology of evolving networks: local events and universality,” *Phys. Rev. Lett.*, vol. 85, no. 24, p. 5234, 2000.
- [39] L. Hébert-Dufresne, J. A. Grochow, and A. Allard, “Multi-scale structure and topological anomaly detection via a new network statistic: the onion decomposition,” *Sci. Rep.*, vol. 6, 2016.
- [40] P. L. Krapivsky, G. J. Rodgers, and S. Redner, “Degree distributions of growing networks,” *Phys. Rev. Lett.*, vol. 86, no. 23, p. 5401, 2001.
- [41] S. N. Dorogovtsev and J. F. F. Mendes, “Scaling behaviour of developing and decaying networks,” *Europhys. Lett.*, vol. 52, no. 1, p. 33, 2000.
- [42] J. S. Liu and R. Chen, “Sequential monte carlo methods for dynamic systems,” *J. Am. Stat. Assoc.*, vol. 93, no. 443, pp. 1032–1044, 1998.
- [43] C. Wiuf, M. Brameier, O. Hagberg, and M. P. Stumpf, “A likelihood approach to analysis of network data,” *Proc. Natl. Acad. Sci. U.S.A.*, vol. 103, no. 20, pp. 7566–7570, 2006.
- [44] S. H. Lee, P.-J. Kim, and H. Jeong, “Statistical properties of sampled networks,” *Phys. Rev. E*, vol. 73, no. 1, p. 016102, 2006.
- [45] L. A. Adamic and B. A. Huberman, “Power-law distribution of the World Wide Web,” *Science*, vol. 287, no. 5461, 2000.
- [46] S. Bubeck, R. Eldan, E. Mossel, M. Z. Rácz, *et al.*, “From trees to seeds: on the inference of the seed from large trees in the uniform attachment model,” *Bernoulli*, vol. 23, no. 4A, pp. 2887–2916, 2017.
- [47] S. B. Seidman, “Network structure and minimum degree,” *Soc. Networks*, vol. 5, no. 3, pp. 269–287, 1983.
- [48] V. Batagelj and M. Zaversnik, “An  $O(m)$  algorithm for cores decomposition of networks,”

- arXiv:cs/0310049*, 2003.
- [49] A. Paranjape, A. R. Benson, and J. Leskovec, “Motifs in temporal networks,” in *Proceedings of the 10th ACM International Conference on Web Search and Data Mining*, pp. 601–610, ACM, 2017.
  - [50] A. Clauset, C. R. Shalizi, and M. E. Newman, “Power-law distributions in empirical data,” *SIAM Rev.*, vol. 51, no. 4, pp. 661–703, 2009.
  - [51] R. Oliveira and J. Spencer, “Connectivity transitions in networks with super-linear preferential attachment,” *Internet Math.*, vol. 2, no. 2, pp. 121–163, 2005.
  - [52] A. D. Broido and A. Clauset, “Scale-free networks are rare,” *arXiv:1801.03400*, 2018.
  - [53] R. Dunbar, “Neocortex size as a constraint on group size in primates,” *J. Hum. Evol.*, vol. 22, no. 6, pp. 469–493, 1992.
  - [54] R. Dunbar, “Social cognition on the internet: testing constraints on social network size,” *Philos. T. R. Soc. B*, vol. 367, no. 1599, pp. 2192–2201, 2012.
  - [55] M. S. Granovetter, “The strength of weak ties,” in *Soc. Networks*, pp. 347–367, Elsevier, 1977.
  - [56] B. Hajek and S. Sankagiri, “Recovering a hidden community in a preferential attachment graph,” *arXiv:1801.06818*, 2018.
  - [57] S. W. Linderman, G. E. Mena, H. Cooper, L. Paninski, and J. P. Cunningham, “Reparameterizing the Birkhoff polytope for variational permutation inference,” *arXiv:1710.09508*, 2017.
  - [58] M. Mezard and A. Montanari, *Information, Physics, and Computation*. Oxford University Press, 2009.
  - [59] A. Y. Lokhov, M. Mézard, H. Ohta, and L. Zdeborová, “Inferring the origin of an epidemic with a dynamic message-passing algorithm,” *Phys. Rev. E*, vol. 90, no. 1, p. 012801, 2014.
  - [60] P. L. Krapivsky and S. Redner, “Statistics of changes in lead node in connectivity-driven networks,” *Phys. Rev. Lett.*, vol. 89, no. 25, p. 258703, 2002.
  - [61] C. Andrieu, N. De Freitas, A. Doucet, and M. I. Jordan, “An introduction to MCMC for machine learning,” *Mach. Learn.*, vol. 50, no. 1-2, 2003.
  - [62] B. H. Erickson, “Some problems of inference from chain data,” *Sociol. Methodol.*, vol. 10, pp. 276–302, 1979.
  - [63] M. S. Handcock and K. J. Gile, “Comment: on the concept of snowball sampling,” *Sociol. Methodol.*, vol. 41, no. 1, pp. 367–371, 2011.
  - [64] H. Jeong, Z. Néda, and A.-L. Barabási, “Measuring preferential attachment in evolving networks,” *Europhys. Lett.*, vol. 61, no. 4, p. 567, 2003.
  - [65] W. H. Press, *Numerical Recipes: The Art of Scientific Computing*. Cambridge University press, 3rd ed., 2007.